Membrane potential (V_{mem}) measurements during mesenchymal stem cell (MSC) proliferation and osteogenic differentiation

Mit Balvantray Bhavsar, Gloria Cato, Alexander Hauschild, Liudmila Leppik, Karla Mychellyne Costa Oliveira, Maria José Eischen-Loges and John Howard Barker

Frankfurt Initiative for Regenerative Medicine, Johann Wolfgang Goethe Universität Frankfurt am Main, Frankfurt am Main, Hessen, Germany

ABSTRACT

Background: Electrochemical signals play an important role in cell communication and behavior. Electrically charged ions transported across cell membranes maintain an electrochemical imbalance that gives rise to bioelectric signaling, called membrane potential or V_{mem}. V_{mem} plays a key role in numerous inter- and intracellular functions that regulate cell behaviors like proliferation, differentiation and migration, all playing a critical role in embryonic development, healing, and regeneration.

Methods: With the goal of analyzing the changes in V_{mem} during cell proliferation and differentiation, here we used direct current electrical stimulation (EStim) to promote cell proliferation and differentiation and simultaneously tracked the corresponding changes in V_{mem} in adipose derived mesenchymal stem cells (AT-MSC).

Results: We found that EStim caused increased AT-MSC proliferation that corresponded to V_{mem} depolarization and increased osteogenic differentiation that corresponded to V_{mem} hyperpolarization. Taken together, this shows that V_{mem} changes associated with EStim induced cell proliferation and differentiation can be accurately tracked during these important cell functions. Using this tool to monitor V_{mem} changes associated with these important cell behaviors we hope to learn more about how these electrochemical cues regulate cell function with the ultimate goal of developing new EStim based treatments capable of controlling healing and regeneration.

Subjects Bioengineering, Cell Biology, Statistics

Keywords Membrane potential, Electrical stimulation, Mesenchymal stem cells, Osteogenic differentiation, Cell proliferation, V_{mem}

Submitted 24 October 2018
Accepted 22 December 2018
Published 8 February 2019

Corresponding authors
Mit Balvantray Bhavsar, mbhavsa@gwdg.de
John Howard Barker, jhb121654@gmail.com

Academic editor
Shi-Cong Tao

Additional Information and Declarations can be found on page 10

DOI **10.7717/peerj.6341**

Copyright
2019 Bhavsar et al.

Distributed under
Creative Commons CC-BY 4.0

OPEN ACCESS

INTRODUCTION

Understanding, harnessing and controlling the body's regenerative capabilities has long been among the most sought-after goals in medical research. Regenerative medicine, by fulfilling its promise of restoring full form and function to tissues and organs, could,

for the first time, make it possible to *cure disease* rather than just treat the symptoms. Stem cells play a, if not the central role in regeneration as well as embryonic development (*Daley, 2015*; *Mahla, 2016*). The signals that regulate these cells are biochemical and/or bioelectric, the latter originating from the passage of positively and negatively charged ions across cell membranes. This active transport of charged ions in and out of cells gives rise to transmembrane voltage gradients or V_{mem}. The V_{mem} across the membrane of cells that are in high proliferative states (embryonic, adult stem cells, cancer cells, etc.) have been shown to trend toward being more positive and are depolarized, while the V_{mem} of cells that are in low proliferative states (neurons, fibroblasts, skeletal muscle cells, fat cells, etc.) are more negative or hyperpolarized (*Stillwell, Cone & Cone, 1973*; *Sundelacruz, Levin & Kaplan, 2008*, *2009*; *Levin, 2012*). During development, these V_{mem} changes across the membrane of embryonic stem cells constitute finely coordinated bioelectric signals that orchestrate embryonic growth throughout development.
The presence and importance of this bioelectric activity on the surface of developing embryos, while poorly understood, has been clearly demonstrated on the surface of developing chick embryos and frog larva. *Shi & Borgens (1995)* measured distinct circular patterns of bioelectric flow around the spinal cords of developing chick embryos. When this electric flow was short circuited by implanting a copper wire adjacent to the electric fields, the chick developed without lower extremities, highlighting the importance of these bioelectric fields in development (*Shi & Borgens, 1995*). In a developing frog larva, *Pai et al. (2015)* chemically disrupted spatial gradients of the transmembrane potential (V_{mem}) and induced forced hyperpolarization by mis-expression of specific ion channels which diminished the expression of early brain markers, causing absent or malformed regions in the embryo's brain and death. In another study, *Lan et al. (2014)* depolarized V_{mem} of cardiac myocytes by adding potassium gluconate or Ouabain to the culture medium and found that depolarization of cardiac myocytes maintains cell proliferation. Also, *Tseng & Levin (2013)* demonstrated that body-wide pharmacological modulation of V_{mem} can induce functional regeneration of the froglet leg at a non-regenerative stage. *Vandenberg, Morrie & Adams (2011)* showed how membrane voltage and pH regionalization are required for craniofacial morphogenesis.
Finally, studying bioelectricity in regeneration *Borgens, Vanable & Jaffe (1977)* were able to measure endogenous bioelectric current emanating from the stumps of amputated, regenerating newt limbs. They found that the intensity of these currents peeked at 4 days post amputation and then gradually subsided over the course of a week. In recent experiments in a rat limb amputation, and separately in a rat femur defect model we demonstrated that physiological levels of externally applied EStim, delivered to limb stumps and bone defects, respectively, significantly increased bone and cartilage regeneration and new vessel formation (*Leppik et al., 2015*, *2018*).

Externally applied EStim has been used clinically to promote bone healing for many years. Only recently have we begun to understand the mechanisms, at a cellular level, by which EStim affects bone healing in this way. In several recent experiments others and we exposed cells, in culture, to externally applied EStim and observed major changes in cell behaviors like, proliferation (*Guo et al., 2012*; *Sebastian et al., 2015*; *Qi et al., 2018*),

differentiation (*Hernández et al., 2016*; *Mobini et al., 2017a*; *Eischen-Loges et al., 2018*), migration (*Jahanshahi et al., 2013*; *Yuan et al., 2014*; *Tai, Tai & Zhao, 2018*) and over-all cell cycle progression (*Griffin et al., 2013*). While changes in endogenous bioelectric activity have been shown to play a crucial role in embryologic development and regeneration, and externally applied EStim has been shown to affect important cell functions involved in regeneration, the role V_{mem} plays in regulating these functions is still poorly understood. To better understand the role of V_{mem} in regeneration-related cell behaviors, in the present study, we used EStim to promote cell proliferation and osteogenic differentiation in adipose-tissue-derived mesenchymal stem cells (AT-MSC) and simultaneously tracked V_{mem} changes over time.

MATERIALS AND METHODS

Groups: Rat AT-MSC were allocated into "cell proliferation" and "osteogenic differentiation" groups. Cells in the proliferation group were cultured in normal medium and were further divided into two groups: Cells that received no EStim (controls) and cells exposed to EStim. Cells in the osteogenic differentiation group were cultured in osteogenic medium and were further divided into two groups: Cells that received no EStim (controls) and cells exposed to EStim. All cells were stained with the membrane potential (V_{mem}) sensitive florescent dye, $DiBAC_4(3)$, and imaged at 0, 7, 14, and 21 days, and cell proliferation and osteogenic differentiation were measured at the same time points.

Cell preparation and culture: Rat AT-MSC were purchased from Cyagen Biosciences (Cat. No. RASMD-01001) and stored in liquid nitrogen at −196 °C, then on the day of the experiment they were thawed, cultured, and expanded to reach the desired number, according to the cell provider's instructions. To achieve the appropriate number, cells were cultured until they reached 80% confluency and then expanded over 6–8 passages. Cells from passage 6–8 were seeded in 6-well cell culture plates (TPP, Trasadingen, Switzerland) at a density of 90,000 cell/cm^2 in cell growth normal medium consisting of Dulbecco's Modified Eagle Medium, GlutaMAX 1 g/L D-Glucose, 10% Fetal Calf Serum, and 1% Penicillin/Streptomycin (10 U/ml), all obtained from GibcoR (Gaithersburg, MD, USA). The seeded 6-well plates were then placed in a humidified incubator at 37 °C with 5% CO_2 and 5% O_2. These cells were used for cell proliferation experiments. For osteogenic differentiation experiments, the cell growth medium in which they had been cultured until this point was replaced with osteogenic cell growth medium, complemented with 10^{-7} M dexamethasone, 10 mM glycerophosphate, and 0.05 mM ascorbic acid-2-phosphate, all obtained from Sigma-Aldrich (Heidelberg, Germany). The culture medium was replaced two times per week.

Electrical stimulation of cells: Electrical stimulation (EStim) was applied by means of a purpose-built DC EStim cell culture chamber described elsewhere (*Mobini, Leppik & Barker, 2016*). Briefly, the EStim chamber consists of a standard 6-well plate with a lid equipped with six pairs of platinum and silver electrodes connected to an electrical power supply (e.g., Triple Output Programmable DC Power Supplier (Supply-Model 9130;

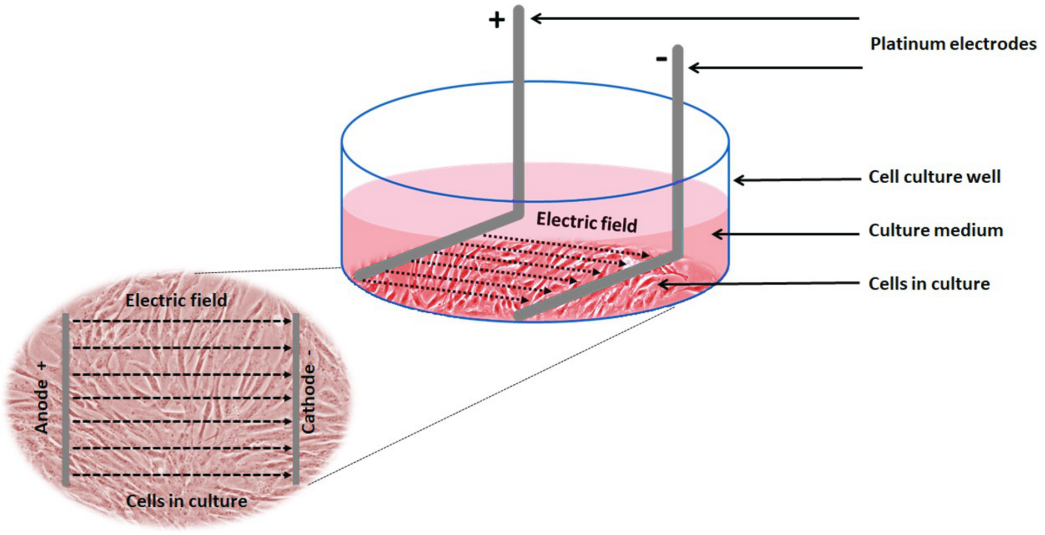

Figure 1 Schematic showing the experimental setup and electric field relative to the cells. Experimental setup showing 1 of 6 wells in our EStim cell culture chamber. AT-MSC seeded in culture medium in a well. L-shaped platinum electrodes, in contact with the bottom of the well, completely immersed in culture medium. Inset image showing cultured cells between anode (+) and cathode (–) in electric field. The image has been edited from (*Mobini et al., 2017a*, *2017b*).

Full-size DOI: 10.7717/peerj.6341/fig-1

B&K Precision, Yorba Linda, CA, USA) (Fig. 1). Using this setup cells were exposed to 100 mV/mm of DC EStim for 1 h/day over the entire duration of the 21-day experiment.

V_{mem} measurements: To visualize and measure V_{mem} changes at the predetermined measurement time points (0, 7, 14, and 21 days) during cell proliferation and osteogenic differentiation, cells were dyed with the anionic voltage-sensitive dye, Bis-(1,3-diethylthiobarbituricacid) trimethine Oxonol ($DiBAC_4(3)$, Invitrogen, Carlsbad, CA, USA), whose uptake by cells is voltage dependent. Higher dye uptake is seen in more depolarized cells (*Sundelacruz, Levin & Kaplan, 2008*; *Dibac, Adams & Levin, 2014*). V_{mem} changes were visualized and measured using fluorescence microscopy, as described by *Adams & Levin (2014)*. For each measurement a fresh solution of 10 mM $DiBAC_4(3)$, in DMSO was prepared and diluted to 0.5 mM in Hank's Buffered Salt Solution (HBSS, Invitrogen, Carlsbad, CA, USA). After adding the dye, the cells were left for 30 min in an incubator at 37 °C, then washed two times using PBS at room temperature and imaged using a Nikon Eclipse Ti-E Inverted Microscope. The $DiBAC_4(3)$ dye was excited with a 420 nm light and the fluorescence images were captured at 520 nm by a non-descanned photomultiplier tube, controlled by NIS Element Software. The captured images were saved as a bright field (BF) image and for every BF image, a flatfield image (FF) (made by defocusing the image) and a dark field (DF) image (made by closing the shutter) were taken. These three images were later used for corrections (see below). All samples were imaged on the same day to minimize time dependent variations. Since fluorescence intensity was quantified for each image, the gain, exposure time, and offset settings of the microscope were kept constant over the duration of each experiment.

Image correction: Image correction was done as previously described (*Adams & Levin, 2012*) using the arithmetic function of NIS Elements imaging software. To correct the images, the corresponding pixels in the three images (BF, FF, DF) were subtracted and a new image of the difference was generated. Each image correction was done as follows:

i. Raw BF image – DF image = DF corrected BF image
ii. FF image – DF image = DF corrected FF image
iii. DF corrected BF image – DF corrected FF image = Corrected final Image

Image quantification: Image quantification was done using NIH's publicly available software, ImageJ. The level of fluorescence of the corrected images was quantified by selecting highly florescent areas within the cell as described in *McCloy et al. (2014)*. Next to these areas, outside the cell an area with no fluorescence was selected to serve as background. Finally, to calculate corrected total fluorescence the following formula was used:

$$\text{Corrected total cell fluorescence (CTCF)} = \text{Integrated density} - (\text{Area of selected cell} * \text{Mean fluorescence of background readings})$$

Cell proliferation: To measure cell proliferation cell number was counted indirectly by estimating dsDNA content according to the Quant-iT TM PicoGreen® dsDNA Reagent and Kits protocol (29851; Molecular Probes, Inc., Eugene, OR, USA) (*Pabbruwe, Stewart & Chaudhuri, 2005*). Briefly, cells were washed two times with PBS, treated with lysis buffer (400 mM potassium phosphate buffer, 2% Triton X100, 10 mM EDTA, pH 7.0), and cell lysates were used for DNA content measurements. A serial dilution of a known amount of AT-MSC was lysed with lysis buffer and used to create a calibration curve showing the correlation between cell number and fluorescence. This latter procedure allowed us to indirectly determine the number of cells in the cultured wells via the calibration curve and measurement with PicoGreen®.

Osteogenic differentiation: Osteogenic differentiation was measured using Alizarin Red that stains calcium deposits in the cells. Cultured cells were washed twice with PBS and fixed with 4% paraformaldehyde (Sigma-Aldrich, München, Germany) solution in PBS for 30 min. Alizarin Red S (Sigma-Aldrich, München, Germany) solution (2% in PBS) was added to the fixed cells, incubated at room temperature for 30 min, and rinsed with deionized water repeatedly. Images were captured with a light microscope (CKX53, CellSens Entry 1.9 Software; Olympus, Tokyo, Japan) at a magnification of 10×. Red color deposits in the images indicate the presence of the complex formed by calcium deposits and the alizarin red. ImageJ Software was used to quantify the intensity of the red color as described in *Camci-Unal et al. (2016)*.

Data analysis and statistics: All experiments were performed in triplicate and Microsoft Excel (2016) was used for all statistical assessments. In most cases, data is presented as the mean value ± standard deviation unless otherwise indicated. The statistical significance

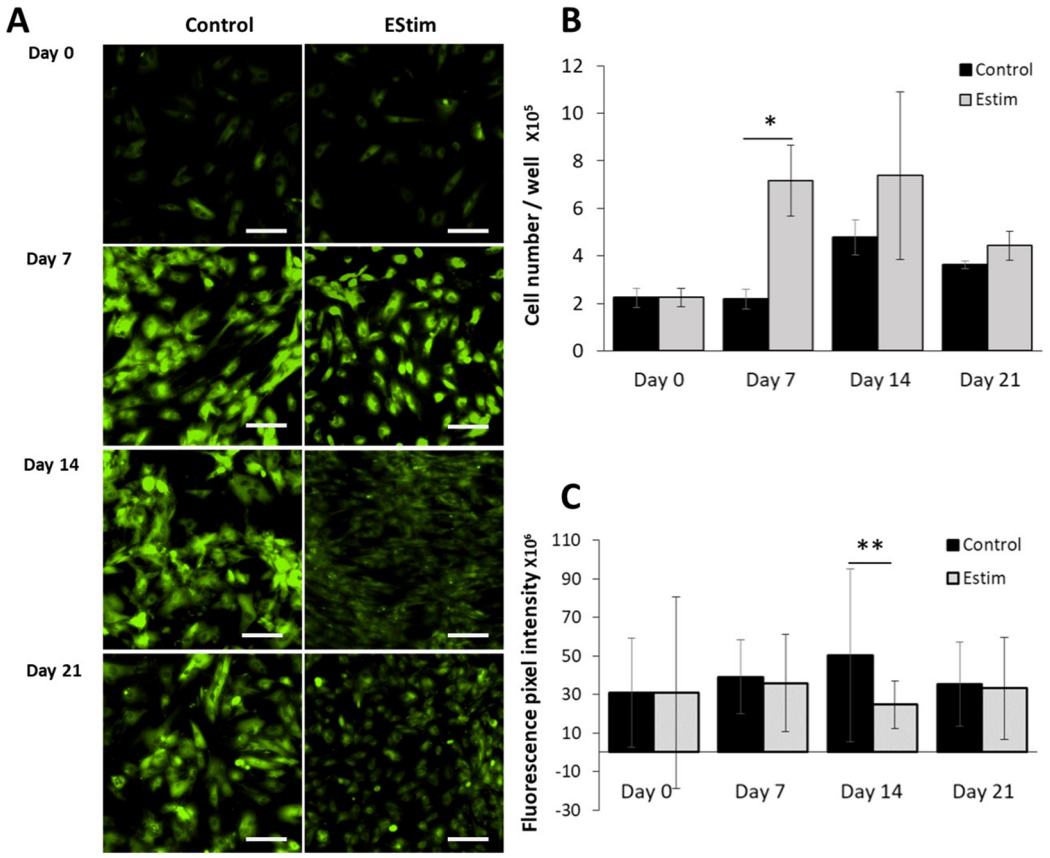

Figure 2 AT-MSC proliferation and V_{mem} measurements. (A) Representative fluorescence images of V_{mem} in EStim-treated and non-treated AT-MSC at days 0, 7, 14, and 21. (B) Graph of proliferation (cell number) of EStim-treated and non-treated AT-MSC at days 0, 7, 14, and 21. (C) Graph of fluorescence intensity (V_{mem}), of EStim-treated and non-treated AT-MSC at days 0, 7, 14, and 21. V_{mem} (fluorescence intensity) was significantly ($p < 0.01$) higher in EStim vs. non-treated AT-MSC at day 14. Bar graphs represent mean pixel intensity with standard deviation ($n = 45$, 5–10 cells/Image from 15 images). Asterisks indicate degree of significant differences between groups at the same time points. $^{*}p < 0.05$, $^{**}p < 0.01$.
Full-size DOI: 10.7717/peerj.6341/fig-2

of differences between groups was analyzed by one-way ANOVA and student *t*-test using Microsoft Excel 2016. Significance level was set at $p < 0.05$.

RESULTS

Cell proliferation and V_{mem} measurements

The cells, used for cell proliferation experiments, were cultured in cell growth normal medium. Cell proliferation and V_{mem} in AT-MSC exposed to, and not (controls) exposed to EStim were measured using PicoGreen® assay and $DiBAC_4(3)$ voltage-sensitive fluorescent dye, respectively (Fig. 2). Proliferation was significantly ($p < 0.05$) increased by 3.5-fold in EStim-treated samples on day 7. It also increased by two-fold, though not significantly, on day 14, and there was no difference between EStim-treated and control cells on day 21 (Fig. 2B). V_{mem} values (fluorescence) were the same as controls on days 7 and 21 and were significantly ($p < 0.01$) decreased in EStim treated cells on day 14 (Figs. 2A right and 2C), and (Figs. 2A left and 2C).

Osteogenic differentiation and V_{mem} measurements

The cells, used for osteogenic differentiation experiments, were cultured in cell growth osteogenic medium. Osteogenic differentiation and changes in V_{mem} in EStim treated and non-treated (control) AT-MSC were measured using Alizarin Red and the voltage-sensitive fluorescent dye $DiBAC_4(3)$ respectively, the results of which are shown in Fig. 3. We found that fluorescence profiles (V_{mem} values) significantly decreased on for day 7 ($p < 0.01$), day 14 ($p < 0.001$) and day 21 ($p < 0.01$) (hyperpolarized) during osteogenic differentiation (Fig. 3A). Accordingly, the EStim treated cells, as the osteogenic differentiation progressed, had lower (less bright) fluorescence profiles than the controls (Figs. 3A, 3C and 3E). The fluorescence profile (V_{mem}) of cells not exposed to EStim (controls) was high at all measurement time points decreasing only on day 21 (Figs. 3A, 3C and 3F). Cells treated with EStim showed an increase in calcium deposits (osteogenic differentiation) already beginning on day 7 and increasing until the end of the experiment, on day 21 (Fig. 3B, right). In cells not receiving EStim (controls), there were little or no calcium deposits at the same measurement time points. We quantified the red color of calcium deposition using ImageJ Software and found that osteogenic differentiation (calcium deposits) was significantly increased at day 14 ($p < 0.001$) and day 21 ($p < 0.001$) in EStim-treated samples (Fig. 3D), and there was no difference between EStim-treated and control cells on day 7 (Fig. 3D).

DISCUSSION

Voltage gradients across the plasma membrane or V_{mem} have been shown to be associated with cell behaviors like cell proliferation (*Blackiston, McLaughlin & Levin, 2009*; *Sundelacruz, Levin & Kaplan, 2009*), differentiation (*Sundelacruz, Levin & Kaplan, 2008*), migration (*McCaig et al., 2005*; *Özkucur et al., 2011*; *Yang & Brackenbury, 2013*) and over-all cell cycle progression, all behaviors that play a crucial role in tissue regeneration (*Sundelacruz, Levin & Kaplan, 2009*). During periods of differentiation, cell V_{mem} has been observed to be hyperpolarized, maintaining values that fluctuate around −90 mV (*Levin, 2011*). As was first shown by Levin et al., cellular differentiation causes hyperpolarized cellular states and as the process of differentiation continues, the cellular population as a whole becomes more hyperpolarized (*Sundelacruz, Levin & Kaplan, 2008*, *2009*).

In recent in vitro studies others (*Gittens et al., 2013*; *Hu et al., 2014*; *Kwon, Lee & Chun, 2016*; *Zhang, Neoh & Kang, 2017*) and we (*Mobini, Leppik & Barker, 2016*; *Mobini et al., 2017a*; *Eischen-Loges et al., 2018*) showed that these same cell behaviors can be induced by exposing cells to externally applied DC EStim. *Zhang, Neoh & Kang (2017)* exposed human AT-MSC to 200 µA of DC EStim for 4 h/day for 7, 14, and 21 days and observed enhanced osteogenic differentiation and increased migration of cells into scaffold material. Similarly, in previous in vitro studies we found that 100 mV/mm of DC EStim for 1 h/day for 7 days stimulated cell proliferation and osteogenic differentiation in bone marrow derived MSC (*Mobini, Leppik & Barker, 2016*; *Mobini et al., 2017a*). In the present study we used EStim to stimulate cell proliferation and osteogenic differentiation in AT-MSC and at the same time tracked V_{mem} changes.

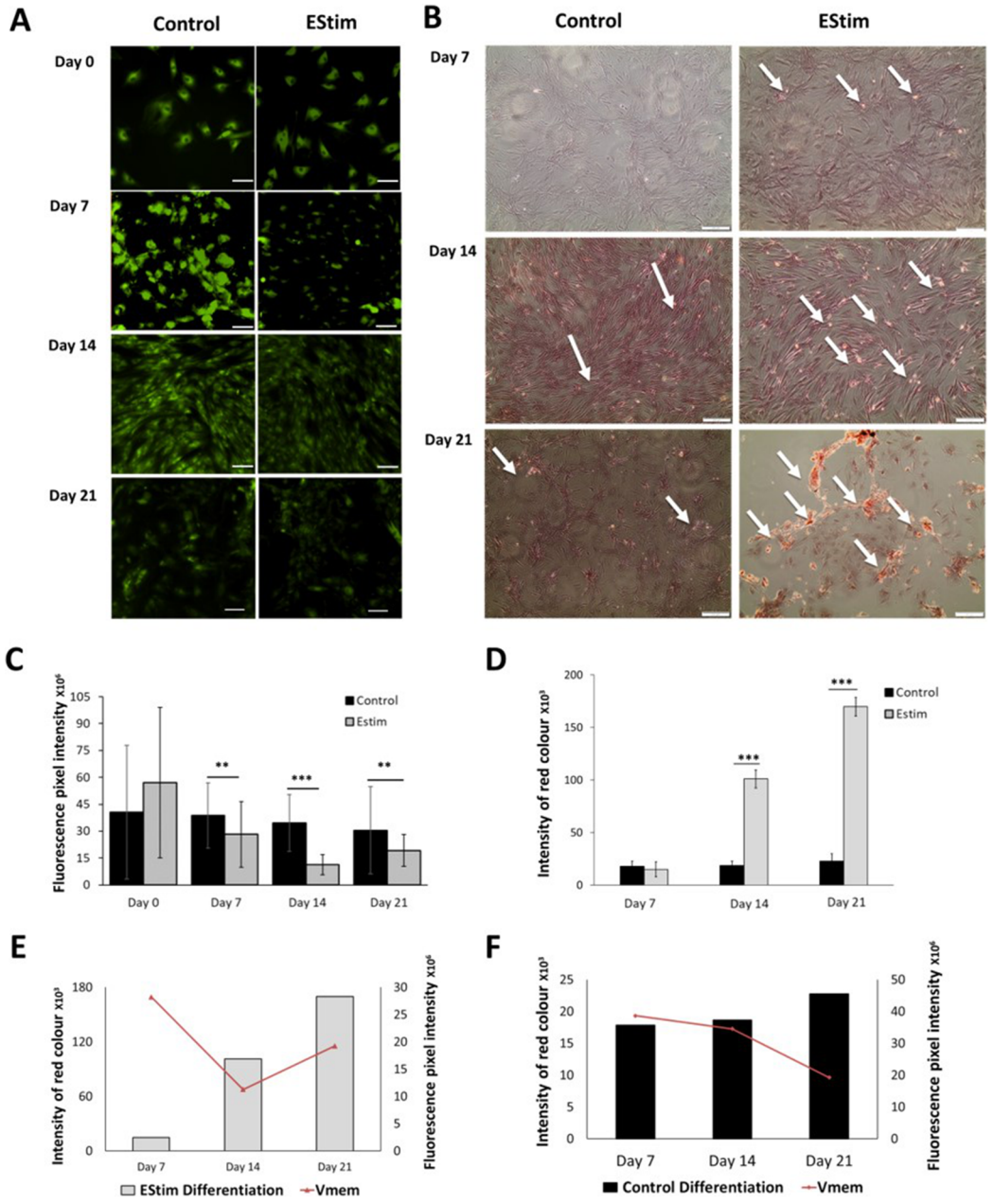

Figure 3 AT-MSC osteogenic differentiation and V_{mem} measurements. (A) Representative fluorescence images of EStim-treated and non-treated AT-MSC during osteogenic differentiation at days 0, 7, 14, and 21. (B) Representative images of Alizarin Red stained calcium deposits in EStim-treated and non-treated AT-MSC during osteogenic differentiation at days 7, 14, and 21. (C) Graph of fluorescence intensity (V_{mem}) values of EStim induced osteogenic differentiation in AT-MSC at days 0, 7, 14, and 21. (D) Graph of intensity of red coloration (calcium deposits) in EStim-treated and non-treated AT-MSC at days 7, 14, and 21. (E) Graph of changes in intensity of red coloration (calcium deposits) (black bars) with superimposed fluorescence intensity (V_{mem}) (red line) in non-treated AT-MSC at days 7, 14, and 21. (F) Graph of changes in intensity of red coloration (calcium deposits) (grey bars) with superimposed fluorescence intensity (V_{mem}) (red line) in EStim-treated AT-MSC at days 7, 14, and 21. Bar graphs represent mean pixel intensity with standard deviation (n = 45, 5–10 cells/Image from 15 images). Asterisks indicate degree of significant differences between groups at the same time points ($^{*}p < 0.05$, $^{**}p < 0.01$, $^{***}p < 0.001$). Full-size DOI: 10.7717/peerj.6341/fig-3

One of the hallmarks of regeneration is cell proliferation. Cell proliferation is a multi-step event regulated by a system of checkpoints at different phases of the cell cycle (*Romar, Kupper & Divito, 2016*). It is known that most non-proliferative cells (e.g., Nerve cells) have hyperpolarized (more negative) V_{mem}, while most proliferative cells (e.g., Cancer cells) have depolarized (less negative) V_{mem} values (*Lan et al., 2014*). Cells are physically transferred to in vitro culture from an in vivo environment using cell extraction techniques, they tend to undergo spontaneous proliferation, which is accompanied by V_{mem} depolarization (*Sundelacruz, Levin & Kaplan, 2009*). In our experiments EStim treated cells showed higher levels of proliferation than non-EStim treated controls at all the measured time points (Fig. 2B). During this period, we tracked V_{mem} of the proliferating AT-MSC and found that values of the EStim treated cells showed no significant decrease, except on day 14 (Fig. 2C). During the same period the non-EStim treated cells showed a similar non-changing pattern and were strongly depolarized (high fluorescence) from days 7 to 21. These observations coincide with those of others who showed that cell proliferation is mostly accompanied by V_{mem} depolarization (*Sundelacruz, Levin & Kaplan, 2009*).

In the present study, as expected we found that in EStim treated cells osteogenic differentiation (calcium deposition by differentiated early osteoblasts) already began on day 7 and continued until day 21 (Fig. 3B). During the same period V_{mem} values were low (hyperpolarized). Taken together with our fluorescence data tracking V_{mem}, we saw that a more negative V_{mem} correlates well with differentiation, as seen in the EStim group. This correlates with findings by others (*Sundelacruz, Levin & Kaplan, 2009*), in which lower V_{mem} values were shown to correlated with higher levels of differentiation. Our findings agree with those of Levin, et al. who found a clear relationship between hyperpolarized cellular states and high levels of cell differentiation. Taken together and compared to both the EStim and control groups, it is clear that AT-MSC hyperpolarization correlates with cell differentiation. Overall, our findings agree with previous work described in the literature (*Sundelacruz, Levin & Kaplan, 2008*). In said experiments by others cell proliferation and differentiation and the corresponding V_{mem} changes were induced using chemical interventions, that is, K^+-ATP-channel openers pinacidil and diazoxide (*Sundelacruz, Levin & Kaplan, 2008*). In contrast, in the present study we used DC EStim to stimulate proliferation and osteogenic differentiation, and also observed the corresponding changes in V_{mem}. The fact that cell proliferation and differentiation and the corresponding V_{mem} changes can be stimulated both chemically (K^+-ATP-channel openers pinacidil and diazoxide), and physically (DC EStim), in the present experiments, indicates that this correlation is robust. While based on this data we cannot say how EStim might affect V_{mem}, in studies by *Valič et al. (2003)* and *Taghian, Narmoneva & Kogan (2015)*, the authors speculate that DC EStim acts on the permeability of the ion channels through which electrically charged molecules pass the cell membrane.

CONCLUSION

In summary, by monitoring V_{mem} signaling during changes in stem cell behaviors we hope to gain a better understanding of the mechanisms by which these electrochemical

cues regulate stem cell function. In future experiments we will determine if the observed V_{mem} changes control proliferation and differentiation in the cells or if it is a consequence of these important cellular functions. This knowledge could lead to the development of new EStim-based therapies that optimize stem cell function in regenerative medicine-based treatments.

ADDITIONAL INFORMATION AND DECLARATIONS

Funding

The work described herein was supported by the Friedrichsheim Foundation (Stiftung Friedrichsheim) in Frankfurt/Main, Germany. The funders had no role in study design, data collection and analysis, decision to publish, or preparation of the manuscript.

Grant Disclosure

The following grant information was disclosed by the authors:
Friedrichsheim Foundation (Stiftung Friedrichsheim) in Frankfurt/Main, Germany.

Competing Interests

The authors declare that they have no competing interests.

Author Contributions

- Mit Balvantray Bhavsar conceived and designed the experiments, performed the experiments, analyzed the data, prepared figures and/or tables and assisted in preparing the manuscript for publication.
- Gloria Cato performed the experiments, analyzed the data.
- Alexander Hauschild prepared figures and/or tables and assisted in preparing the manuscript for publication.
- Liudmila Leppik conceived and designed the experiments, contributed reagents/materials/analysis tools, assisted in preparing the manuscript for publication.
- Karla Mychellyne Costa Oliveira assisted in preparing the manuscript for publication.
- Maria José Eischen-Loges performed the experiments.
- John Howard Barker edited and corrected the manuscript.

Data Availability

The following information was supplied regarding data availability:

The raw measurements are available in the Supplemental Files 1 and 2. Figure 2 shows raw data regarding AT-MSC proliferation and Fig. 3 regarding AT-MSC osteogenic differentiation.

Supplemental Information

Supplemental information for this article can be found online at http://dx.doi.org/10.7717/peerj.6341#supplemental-information.

REFERENCES

Adams DS, Levin M. 2012. Measuring resting membrane potential using the fluorescent voltage reporters DiBAC4(3) and CC2-DMPE. *Cold Spring Harbor Protocols* **2012(4)**:459–464 DOI 10.1101/pdb.prot067702.

Adams DS, Levin M. 2014. General principles for measuring resting membrane potential and ion concentration using fluorescent bioelectricity reporters. *Cold Spring Harbor Protocols* **2012(4)**:385–397 DOI 10.1101/pdb.top067710.General.

Blackiston DJ, McLaughlin KA, Levin M. 2009. Bioelectric controls of cell proliferation: ion channels, membrane voltage and the cell cycle. *Cell Cycle* **8(21)**:3527–3536 DOI 10.4161/cc.8.21.9888.

Borgens RB, Vanable JW, Jaffe LF. 1977. Bioelectricity and regeneration. I. Initiation of frog limb regeneration by minute currents. *Journal of Experimental Zoology* **200(3)**:403–416 DOI 10.1002/jez.1402000310.

Camci-Unal G, Laromaine A, Hong E, Derda R, Whitesides GM. 2016. Biomineralization guided by paper templates. *Scientific Reports* **6(1)**:27693 DOI 10.1038/srep27693.

Daley GQ. 2015. Stem cells and the evolving notion of cellular identity. *Philosophical Transactions of the Royal Society B: Biological Sciences* **370(1680)**:20140376 DOI 10.1098/rstb.2014.0376.

Dibac VR, Adams DS, Levin M. 2014. Measuring resting membrane potential using the fluorescent voltage reporters DiBAC4 (3) and CC2-DMPE. *Cold Spring Harbor Protocols* **2012(4)**:459–464 DOI 10.1101/pdb.prot067702.Measuring.

Eischen-Loges M, Oliveira KMC, Bhavsar MB, Barker JH, Leppik L. 2018. Pretreating mesenchymal stem cells with electrical stimulation causes sustained long-lasting pro-osteogenic effects. *PeerJ* **6**:e4959 DOI 10.7717/peerj.4959.

Gittens RA, Olivares-Navarrete R, Rettew R, Butera RJ, Alamgir FM, Boyan BD, Schwartz Z. 2013. Electrical polarization of titanium surfaces for the enhancement of osteoblast differentiation. *Bioelectromagnetics* **34(8)**:599–612 DOI 10.1002/bem.21810.

Griffin M, Sebastian A, Colthurst J, Bayat A. 2013. Enhancement of differentiation and mineralisation of osteoblast-like cells by degenerate electrical waveform in an in vitro electrical stimulation model compared to capacitive coupling. *PLOS ONE* **8(9)**:e72978 DOI 10.1371/journal.pone.0072978.

Guo BS, Cheung KK, Yeung SS, Zhang BT, Yeung EW. 2012. Electrical stimulation influences satellite cell proliferation and apoptosis in unloading-induced muscle atrophy in mice. *PLOS ONE* DOI 10.1371/journal.pone.0030348.

Hernández D, Millard R, Sivakumaran P, Wong RCB, Crombie DE, Hewitt AW, Liang H, Hung SSC, Pébay A, Shepherd RK, Dusting GJ, Lim SY. 2016. Electrical stimulation promotes cardiac differentiation of human induced pluripotent stem cells. *Stem Cells International* DOI 10.1155/2016/1718041.

Hu WW, Hsu YT, Cheng YC, Li C, Ruaan RC, Chien CC, Chung CA, Tsao CW. 2014. Electrical stimulation to promote osteogenesis using conductive polypyrrole films. *Materials Science and Engineering: C* **37**:28–36 DOI 10.1016/j.msec.2013.12.019.

Jahanshahi A, Schonfeld L, Janssen MLF, Hescham S, Kocabicak E, Steinbusch HWM, Van Overbeeke JJ, Temel Y. 2013. Electrical stimulation of the motor cortex enhances progenitor cell migration in the adult rat brain. *Experimental Brain Research* **231(2)**:165–177 DOI 10.1007/s00221-013-3680-4.

Kwon HJ, Lee GS, Chun H. 2016. Electrical stimulation drives chondrogenesis of mesenchymal stem cells in the absence of exogenous growth factors. *Scientific Reports* **6(1)**:39302 DOI 10.1038/srep39302.

Lan JY, Williams C, Levin M, Black LD. 2014. Depolarization of cellular resting membrane potential promotes neonatal cardiomyocyte proliferation in vitro. *Cellular and Molecular Bioengineering* **7(3)**:432–445 DOI 10.1007/s12195-014-0346-7.

Leppik LP, Froemel D, Slavici A, Ovadia ZN, Hudak L, Henrich D, Marzi I, Barker JH. 2015. Effects of electrical stimulation on rat limb regeneration, a new look at an old model. *Scientific Reports* **5(1)**:18353 DOI 10.1038/srep18353.

Leppik L, Zhihua H, Mobini S, Thottakkattumana Parameswaran V, Eischen-Loges M, Slavici A, Helbing J, Pindur L, Oliveira KMC, Bhavsar MB, Hudak L, Henrich D, Barker JH. 2018. Combining electrical stimulation and tissue engineering to treat large bone defects in a rat model. *Scientific Reports* **8(1)**:6307 DOI 10.1038/s41598-018-24892-0.

Levin M. 2011. Endogenous bioelectric signals as morphogenetic controls of development, regeneration and neoplasm. In: Pullar C, ed. *The Physiology of Bioelectricity in Development, Tissue Regeneration and Cancer*. Boca Raton: CRC Press, 49.

Levin M. 2012. Molecular bioelectricity in developmental biology: new tools and recent discoveries. *BioEssays* **34(3)**:205–217 DOI 10.1002/bies.201100136.

Mahla RS. 2016. Stem cells applications in regenerative medicine and disease therapeutics. *International Journal of Cell Biology* **2016**:1–24 DOI 10.1155/2016/6940283.

McCaig CD, Rajnicek AM, Song B, Zhao M. 2005. Controlling cell behavior electrically: current views and future potential. *Physiological Reviews* **85(3)**:943–978 DOI 10.1152/physrev.00020.2004.

McCloy RA, Rogers S, Caldon CE, Lorca T, Castro A, Burgess A. 2014. Partial inhibition of Cdk1 in G2phase overrides the SAC and decouples mitotic events. *Cell Cycle* **13(9)**:1400–1412 DOI 10.4161/cc.28401.

Mobini S, Leppik L, Barker JH. 2016. Direct current electrical stimulation chamber for treating cells in vitro. *BioTechniques* **60(2)**:95–98 DOI 10.2144/000114382.

Mobini S, Leppik L, Thottakkattumana Parameswaran V, Barker JH. 2017a. In vitro effect of direct current electrical stimulation on rat mesenchymal stem cells. *Peerj* **5**:e2821 DOI 10.7717/peerj.2821.

Mobini S, Talts Ü-L, Xue R, Cassidy NJ, Cartmell SH. 2017b. Electrical stimulation changes human mesenchymal stem cells orientation and cytoskeleton organization. *Journal of Biomaterials and Tissue Engineering* **7(9)**:829–833 DOI 10.1166/jbt.2017.1631.

Özkucur N, Perike S, Sharma P, Funk RHW. 2011. Persistent directional cell migration requires ion transport proteins as direction sensors and membrane potential differences in order to maintain directedness. *BMC Cell Biology* **12(1)**:4 DOI 10.1186/1471-2121-12-4.

Pabbruwe MB, Stewart K, Chaudhuri JB. 2005. A comparison of colorimetric and DNA quantification assays for the assessment of meniscal fibrochondrocyte proliferation in microcarrier culture. *Biotechnology Letters* **27(19)**:1451–1455 DOI 10.1007/s10529-005-1308-x.

Pai VP, Lemire JM, Pare J-F, Lin G, Chen Y, Levin M. 2015. Endogenous gradients of resting potential instructively pattern embryonic neural tissue via notch signaling and regulation of proliferation. *Journal of Neuroscience* **35(10)**:4366–4385 DOI 10.1523/JNEUROSCI.1877-14.2015.

Qi Z, Xia P, Pan S, Zheng S, Fu C, Chang Y, Ma Y, Wang J, Yang X. 2018. Combined treatment with electrical stimulation and insulin-like growth factor-1 promotes bone regeneration in vitro. *PLOS ONE* **13(5)**:e0197006 DOI 10.1371/journal.pone.0197006.

Romar GA, Kupper TS, Divito SJ. 2016. Research techniques made simple: techniques to assess cell proliferation. *Journal of Investigative Dermatology* **136(1)**:e1–e7 DOI 10.1016/j.jid.2015.11.020.

Sebastian A, Iqbal SA, Colthurst J, Volk SW, Bayat A. 2015. Electrical stimulation enhances epidermal proliferation in human cutaneous wounds by modulating p53-SIVA1 interaction. *Journal of Investigative Dermatology* DOI 10.1038/jid.2014.502.

Shi R, Borgens RB. 1995. Three-dimensional gradients of voltage during development of the nervous system as invisible coordinates for the establishment of embryonic pattern. *Developmental Dynamics* **202(2)**:101–114 DOI 10.1002/aja.1002020202.

Stillwell EF, Cone CM, Cone CD. 1973. Stimulation of DNA synthesis in CNS neurones by sustained depolarisation. *Nature New Biology* **246(152)**:110–111 DOI 10.1038/newbio246110a0.

Sundelacruz S, Levin M, Kaplan DL. 2008. Membrane potential controls adipogenic and osteogenic differentiation of mesenchymal stem cells. *PLOS ONE* **3(11)**:e3737 DOI 10.1371/journal.pone.0003737.

Sundelacruz S, Levin M, Kaplan DL. 2009. Role of membrane potential in the regulation of cell proliferation and differentiation. *Stem Cell Reviews and Reports* **5(3)**:231–246 DOI 10.1007/s12015-009-9080-2.

Taghian T, Narmoneva DA, Kogan AB. 2015. Modulation of cell function by electric field: A high-resolution analysis. *Journal of the Royal Society Interface* **12(107)**:20150153 DOI 10.1098/rsif.2015.0153.

Tai G, Tai M, Zhao M. 2018. Electrically stimulated cell migration and its contribution to wound healing. *Burns & Trauma* **6(1)**:20 DOI 10.1186/s41038-018-0123-2.

Tseng A, Levin M. 2013. Cracking the bioelectric code: Probing endogenous ionic controls of pattern formation. *Communicative & Integrative Biology* **6(1)**:e22595 DOI 10.4161/cib.22595.

Valič B, Golzio M, Pavlin M, Schatz A, Faurie C, Gabriel B, Teissié J, Rols MP, Miklavčič D. 2003. Effect of electric field induced transmembrane potential on spheroidal cells: Theory and experiment. *European Biophysics Journal* **32(6)**:519–528 DOI 10.1007/s00249-003-0296-9.

Vandenberg LN, Morrie RD, Adams DS. 2011. V-ATPase-dependent ectodermal voltage and Ph regionalization are required for craniofacial morphogenesis. *Developmental Dynamics* **240(8)**:1889–1904 DOI 10.1002/dvdy.22685.

Yang M, Brackenbury WJ. 2013. Membrane potential and cancer progression. *Frontiers in Physiology* DOI 10.3389/fphys.2013.00185.

Yuan X, Arkonac DE, Chao PHG, Vunjak-Novakovic G. 2014. Electrical stimulation enhances cell migration and integrative repair in the meniscus. *Scientific Reports* **4(1)**:3674 DOI 10.1038/srep03674.

Zhang J, Neoh KG, Kang ET. 2017. Electrical stimulation of adipose-derived mesenchymal stem cells and endothelial cells co-cultured in a conductive scaffold for potential orthopaedic applications. *Journal of Tissue Engineering and Regenerative Medicine* **12(4)**:878–889 DOI 10.1002/term.2441.